Proc. Natl. Acad. Sci. USA
Vol. 80, pp. 5289–5293, September 1983
Biophysics

Crystal structures of the active site in specifically metal-depleted and cobalt-substituted horse liver alcohol dehydrogenase derivatives

(metalloenzymes/x-ray crystallography)

GUNTER SCHNEIDER*†, HANS EKLUND†, EILA CEDERGREN-ZEPPEZAUER†, AND MICHAEL ZEPPEZAUER*‡

†Department of Chemistry and Molecular Biology, Swedish University of Agricultural Sciences, S-750 07 Uppsala, Sweden; and *Fachbereich 15, Analytische und Biologische Chemie, Universität des Saarlandes, D-6600 Saarbrücken 11, Federal Republic of Germany

Communicated by William N. Lipscomb, February 7, 1983

ABSTRACT **Two derivatives of horse liver alcohol dehydrogenase (LADH) in which the active site is specifically metal-depleted [$H_4Zn(n)_2$LADH] or specifically Co-substituted [$Co(c)_2Zn(n)_2$LADH] have been studied by crystallographic methods. (In these formulae, "n" identifies the noncatalytic zinc ion and "c" identifies the catalytic metal ion.) X-ray data were collected for $H_4Zn(n)_2$LADH to 2.7-Å resolution and for $Co(c)_2Zn(n)_2$LADH to 2.4-Å resolution. Difference Fourier maps demonstrate clearly that the catalytic zinc ions are removed in $H_4Zn(n)_2$LADH, whereas the noncatalytic zinc ions are still present. A 2.5-Å shift in the sulphur position of cysteine-46 and a slight torsion of the imidazole ring of histidine-67 are the only changes in the protein structure that could be detected when compared to the native zinc enzyme. The structure of $Co(c)_2Zn(n)_2$LADH is essentially the same as that of the native enzyme. Each cobalt ion is bound to the ligands cysteine-46, cysteine-174, and histidine-67 and to a water molecule in a distorted tetrahedral geometry. A slight change in the position of histidine-67 was found. No further structural changes could be observed in the protein.**

Much effort has been devoted to the selective replacement of zinc ions in the dimeric enzyme horse liver alcohol dehydrogenase (LADH) by other metal ions suitable as spectroscopic probes. The first successful attempts consisted of exchange dialysis techniques developed by Vallee and co-workers that led to the preparation of well-defined species of the general composition Me_2Zn_2LADH or Me_4LADH, where Me denotes Co(II), Cd(II), or ^{65}Zn(II) ions (1–4). Because LADH [and probably also alcohol dehydrogenase (ADH) from yeast] contains two different zinc binding sites per subunit (namely, one catalytic and one noncatalytic site), the assignment of the replaced metal ions with respect to location and properties has long been a matter of controversy (for a summary, see ref. 5).

These controversies have been settled by an exchange technique that is based on the selective removal of the catalytic zinc ions in LADH by treatment of a crystal suspension with chelating agents (6). Subsequent addition of metal ions to the crystal suspension or to a solution of the apo-Zn enzyme under carefully controlled conditions leads to metallo-LADH of the general composition $Me(c)_2Zn(n)_2$LADH, where "n" identifies the noncatalytic zinc ion and "c" identifies the catalytic metal ion. So far, well-defined derivatives have been prepared with Me = Co(II) (6), Cu(II) and Cu(I) (7), Ni(II) (8), and Cd(II) (9).

Because cobalt-substituted LADHs have been frequently used as suitable models for the native zinc enzyme (10–13), we have undertaken an x-ray crystallographic study of $Co(c)_2Zn(n)_2$LADH. Furthermore, $H_4Zn(n)_2$LADH has been included in this study for two reasons. First, it will prove the selective removal of the zinc ion from the catalytic site, which is the critical step of the preparation of all active-site specifically substituted metallo-ADHs. Second, the catalytic metal ion has been shown to participate in the catalytic cycle in at least two ways: it directly binds and activates the substrate by inner-sphere coordination (14) and indirectly influences the mechanism of coenzyme binding because the rates of association and dissociation of coenzyme are dependent on the kind of metal present in the catalytic site (15). Therefore, $H_4Zn(n)_2$LADH is not only interesting as a crucial intermediate but also will offer the possibility of further investigation of the structural changes accompanying the binding of coenzyme and the influence of the catalytic metal ion in the coenzyme-induced conformational change in LADH.

MATERIAL AND METHODS

LADH was purchased in the Federal Republic of Germany from Boehringer Mannheim; Tris, from Serva (Heidelberg); and dipicolinic acid, from Sigma (Munich). All chemicals were of the purest grade commercially available. Doubly distilled water was used throughout, and all solutions were kept free of oxygen by flushing with nitrogen. Glassware was cleaned with concentrated HNO_3 and rinsed extensively with water. All steps in the preparation of crystals and data collection were performed in a cold room at 4°C. LADH was recrystallized at pH 8.4 in 0.05 M Tris with *t*-butyl alcohol (20%, vol/vol) as precipitant. The removal of the catalytic zinc ions with dipicolinic acid and the preparation of $Co(c)_2Zn(n)_2$LADH was performed in the crystalline state as described by Maret *et al.* (6). The metal content of the different crystal species used for the x-ray experiments was determined on a Perkin-Elmer 400 atomic absorption spectrophotometer. The zinc content of $H_4Zn(n)_2$LADH and $Co(c)_2Zn(n)_2$LADH was 1.8–2.0 mol of zinc per dimer. The cobalt content of $Co(c)_2Zn(n)_2$LADH was determined to 1.6 mol of cobalt per dimer. Activity measurements of dissolved crystals have been performed by the method of Dalziel (16). The specific activity of $H_4Zn(n)_2$LADH was 0.1–0.5% of the native enzyme, whereas the specific activity of $Co(c)_2Zn(n)_2$LADH reached 50% of the native enzyme. Because there was too much convection in the mother liquid during the mounting of crystals into glass capillaries, the precipitant *t*-butyl alcohol was exchanged by stepwise dialysis against 0.05 M Tris (pH 8.4) and

The publication costs of this article were defrayed in part by page charge payment. This article must therefore be hereby marked "*advertisement*" in accordance with 18 U.S.C. §1734 solely to indicate this fact.

Abbreviations: ADH, alcohol dehydrogenase; LADH, horse liver alcohol dehydrogenase; c and n in formulae, the catalytic metal ion is denoted by "c" after the chemical symbol of the metal, and the noncatalytic metal ion is denoted by "n"; thus, $H_4Zn(n)_2$LADH is LADH depleted of the catalytic metal ions and $Co(c)_2Zn(n)_2$LADH is LADH in which the catalytic zinc ions are replaced by cobalt.

‡To whom reprint requests should be addressed.

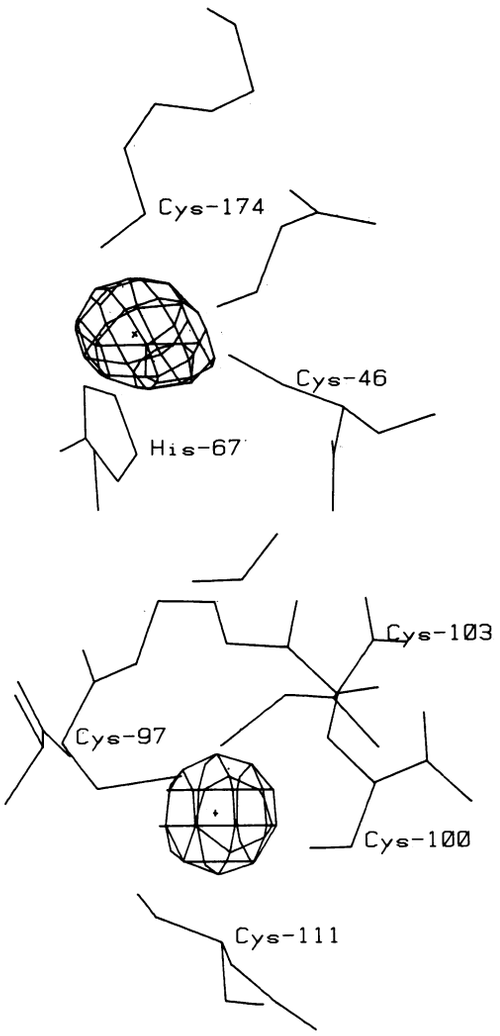

FIG. 1. (*a*) Minimum in the electron density at the catalytic site of $H_4Zn(n)_2$LADH. Difference Fourier map with coefficients ($|F_{obs}| - |F_c|$), where F_{obs} is obtained for the native enzyme $Zn(c)_2Zn(n)_2$LADH. The negative contour level shown here is 8 times the standard deviation of the map. The position of the catalytic zinc ion in the native enzyme subunit is marked by × [crystallographically, both subunits are identical (17)]. (*b*) Peak at the noncatalytic metal-binding site of $H_4Zn(n)_2$LADH; difference Fourier map with coefficients ($|F_{obs}| - |F_c|$), where the contribution of the zinc ions has been excluded from the structure factor calculation. The contour level shown here is 10 times the standard deviation of the map. The position of the metal ion is marked by +.

2-methyl-2,4-pentanediol, until the final concentration of this precipitant reached 25% (vol/vol).

X-ray data were collected on a Stoe computer-controlled four-circle diffractometer according to procedures described in detail earlier (17). Eleven orthorhombic crystals of $H_4Zn(n)_2$LADH were used to collect the 12,340 reflections corresponding to a 2.7-Å resolution, and 18 crystals of $Co(c)_2Zn(n)_2$LADH were used to collect the 15,502 reflections corresponding to a 2.4-Å resolution. The crystals belong to the space group $C222_1$, with one subunit per asymmetric unit. Corrections were applied for the Lorentz and polarization effects, absorption effects (18), and the time-dependent decrease in intensity due to radiation damage. A rough scale for the F values from the different crystals was determined from 30 selected reflections that were measured on all crystals. The F values for each crystal were finally scaled (19) against the corresponding F values from the native

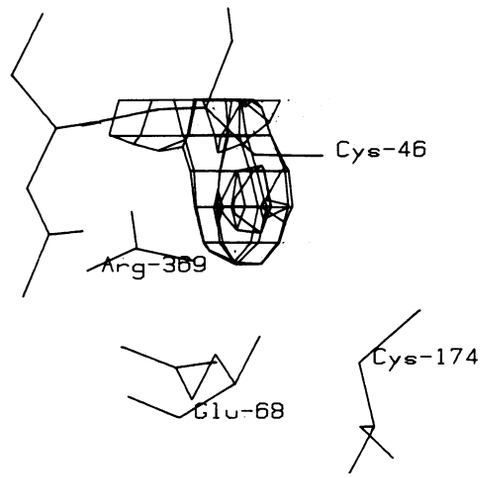

FIG. 2. Region around cysteine-46 from a ($|F_{obs}| - |F_c|$) map of $H_4Zn(n)_2$LADH, with calculated phases in which cysteine-46, cysteine-174, histidine-67, and the zinc ions were excluded from the F_c calculation. The native enzyme model is superimposed on the difference map and illustrates that the position of the sulphur of cysteine-46 does not coincide with the difference density.

protein data. These observed structure factors were combined with phases calculated with PROTEIN (W. Steigemann, Max Planck-Institut für Biochemie, Martinsried, Federal Republic of Germany) from a recently refined model of the orthorhombic structure, which at present has a crystallographic R value of 21% (T. A. Jones, personal communication). Difference electron density maps were calculated with coefficients ($|F_{obs}| - |F_c|$) and ($2|F_{obs}| - |F_c|$), where F_{obs} denotes the observed F values for the derivative and F_c denotes the calculated structure factors from the refined model. Furthermore, difference Fourier maps using structure factors, where the contributions of the catalytic and noncatalytic metal ions and of the protein ligands of the catalytic metal ion—cysteine-46, histidine-67, and cysteine-174—have been excluded, were used to detect changes in ligand geometry and metal distribution. Final positioning of the ligands of the active-site metal was done from these maps. All maps were examined in a Vector General 3404 interactive graphics display by the RING and FRODO programs (20, 21).

RESULTS

$H_4Zn(n)_2$LADH. The most significant feature in the ($|F_{obs}| - |F_c|$) electron density map of the subunit calculated from the $H_4Zn(n)_2$LADH data was a deep minimum in electron density approximately 15 times the standard deviation at the position of the catalytic zinc ion (Fig. 1*a*). No significant difference in electron density was detected at the position of the noncatalytic metal ion. From this map, it was clear that the noncatalytic zinc is present to the same extent as in the native enzyme, whereas the active site has been depleted of zinc. In order to evaluate more quantitatively the average amount of zinc still present at the active site, a difference map was calculated in which the contributions of both metal ions and the ligands for the catalytic metal ion were excluded from the calculated structure factors and phases. In such a map, maxima should appear at the positions of the excluded metal atoms if they are present in the structure, and the height of each maximum is related to the average occupancy of the zinc site.

The electron density found at the position of the catalytic zinc was less than 1 standard deviation, whereas at the position of the noncatalytic zinc, a maximum of approximately 15 times the standard deviation appeared (Fig. 1*b*). These results show

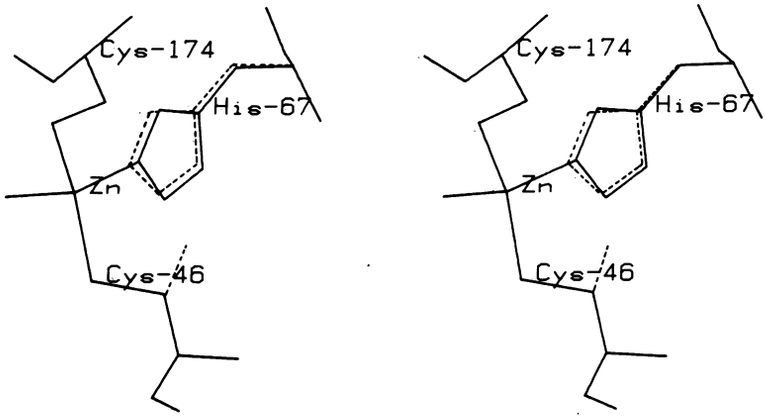

FIG. 3. Stereodiagram of the metal-depleted catalytic site of $H_4Zn(n)_2$LADH compared to the native protein. ——, Native protein; ---, $H_4Zn(n)_2$LADH.

clearly that in the $H_4Zn(n)_2$LADH dimer, the catalytic metal ions are completely removed, whereas the noncatalytic zinc sites are still fully occupied and not affected by the treatment of crystals with dipicolinic acid.

Because $H_4Zn(n)_2$LADH crystals could be stored for weeks during these studies, the x-ray analysis proves that a migration of the structural zinc ions to the metal-depleted active sites does not take place in the crystalline state. This is consistent with the observation (6) that no significant increase in activity occurs on prolonged storage of the crystals of $H_4Zn(n)_2$LADH.

The maps showed only a few other significant differences in electron density, all situated in or nearby the catalytic site region of $H_4Zn(n)_2$LADH. Among these, a change of the sulphur position of cysteine-46 is the most significant one. The difference maps clearly showed that the sulphur atom was out of density, and a maximum was found 2.5 Å from its original position (Fig. 2). The sulphur could be placed in this density by applying a torsion of 70° around the C^{α}—C^{β} bond of cysteine-46. The maps showed a less pronounced shift of histidine-67, which is interpreted in terms of a movement of the imidazole ring of histidine-67 away from the active site.

Thus, the total change in the ligand sphere after the removal of the catalytic zinc ion can be described as a widening of the former metal binding site, which involves cysteine-46 and histidine-67. Cysteine-174 remains in the same position as in the native structure (Fig. 3). As a consequence of the opening of the site in the absence of the metal, the sulphur–sulphur distance increases from 4 to 4.5 Å. Thus, a disulfide bridge between cysteine-46 and cysteine-174 can be excluded. The relatively large movement of cysteine-46 decreases the distance to the closest carboxyl oxygen of glutamic acid-68 to 3.1 Å, indicating a possible hydrogen bond between these two residues. Slight changes for the carboxyl group of glutamic acid-68 and for the guanidinium group of arginine-369 were observed.

$Co(c)_2Zn(n)_2$LADH. A ($|F_{obs}| - |F_c|$) Fourier map with the $Co(c)_2Zn(n)_2$LADH data, where the metal atoms had been removed from the F_c calculation, showed maxima at both the catalytic (Fig. 4) and the noncatalytic metal positions. From the ratio of the peak heights (about 20 times the standard deviation at the noncatalytic metal site and 15 times the standard deviation at the catalytic metal site), a substitution degree at the active site of approximately 75% can be evaluated. This value agrees well with the cobalt content of 1.6 mol per dimer $Co(c)_2$-$Zn(n)_2$LADH (equals 80% substitution) determined by atomic absorption spectroscopy.

A ($|F_{obs}| - |F_c|$) map with contributions of the zinc atoms included in the native structure factors and phases showed no change in electron density at the noncatalytic site and a minimum (about 5 times the standard deviation) at the catalytic metal position.

The center of electron density of the cobalt ion at the catalytic site is slightly shifted from the position of the zinc ion in the native protein. The ($|F_{obs}| - |F_c|$) map, where the metal atoms and the ligands cysteine-46, histidine-67, and cysteine-174 have been excluded from the F_c calculation, showed that cysteine-46 and cysteine-174 fitted in the center of its electron density. Only the imidazole ring of histidine-67 had to be moved slightly (Fig. 5).

In the native LADH, the catalytic zinc ion is coordinated to these three protein ligands and, depending on pH, one water molecule or hydroxyl ion (22). Because the contribution of this water molecule is not included in the native phases, it should appear as a peak in a difference Fourier map. In the difference electron density map of the $Co(c)_2Zn(n)_2$LADH, a significant maximum (about 5 times the standard deviation) appeared at the position of the metal-bound water molecule (Fig. 6). This peak is interpreted as cobalt-bound water. Thus, the cobalt ion in $Co(c)_2Zn(n)_2$LADH is bound in a distorted tetrahedral ge-

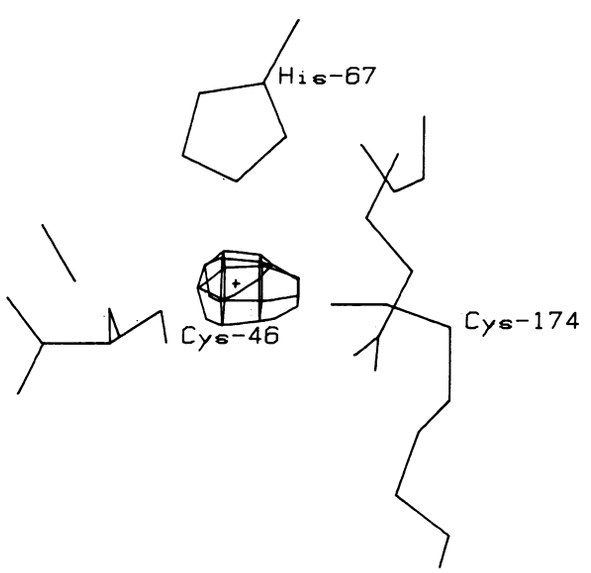

FIG. 4. Peak in the catalytic site of $Co(c)_2Zn(n)_2$LADH from a map with coefficients ($|F_{obs}| - |F_c|$), where the contributions of the metal ions have been excluded from the F_c calculation. The contour level shown here is 10 times the standard deviation. The position of the cobalt ion is marked by +.

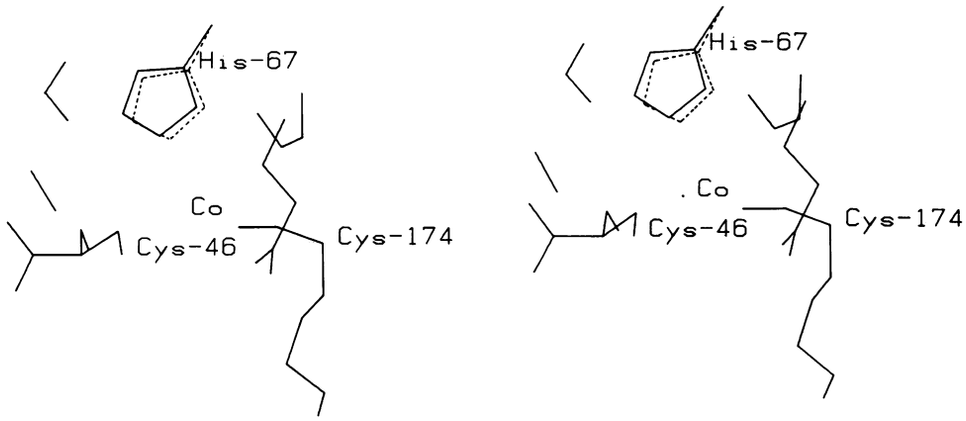

FIG. 5. Stereodiagram of the catalytic site of $Co(c)_2Zn(n)_2$LADH (---) superimposed on the native structure (——).

ometry to the same ligands as the zinc ion in the native protein (Table 1). No further significant changes in the protein structure could be detected in the difference Fourier maps.

DISCUSSION

The present investigation has helped to clarify three important aspects concerning the properties and function of the catalytic metal ion and its environment in LADH. First, the assignment of native and exchanged metal ions to their respective binding sites was definitely established. Thus, the selective replacement of the catalytic zinc ion by the extraction–insertion technique of Maret *et al.* (6) and the selective replacement of the noncatalytic zinc ion by the dialysis techniques of Vallee *et al.* (1–4) and others (6, 10) provide specific methods for preparing a variety of well-defined metal–zinc hybrid LADHs useful for enzymatic and physicochemical studies. In particular, the unambiguous assignment of the exchanged metal ions to their binding sites removes the necessity of using fully substituted metallo-LADHs (5) in those studies where the specific function of the catalytic metal ion is to be studied. Thus, the interpretation of spectroscopic data is greatly simplified.

Second, the investigation of the metal-depleted species $H_4Zn(n)_2$LADH sheds light on the importance of the protein structure for the coordination geometry that the catalytic metal ion acquires in its binding site. The three protein ligands cysteine-46, histidine-67, and cysteine-174 originate from rather distant loci along the polypeptide chain. The backbones of these three amino acids are incorporated in well-ordered helices and β sheets. This may be the reason why removal of the zinc ion does not lead to gross structural changes of tertiary structure, although data from solution seem to support a structure-stabilizing role of the catalytic metal ion (6). The rigidity of the protein structure of $H_4Zn(n)_2$LADH, including its metal-binding site, is obviously responsible for the fact that, in metallo-LADHs, tetrahedral coordination is observed with metals that tend to prefer planar coordination geometries, such as Cu(II) and Ni(II) ions (7, 8). Thus, LADH may be expected to represent a macromolecular ligand system that generally imposes tetrahedral coordination geometries on those metal ions that can form stable complexes with the ligand.

Finally, this conclusion is supported firmly by the present x-ray investigation of $Co(c)_2Zn(n)_2$LADH. The catalytic site of this species is highly similar to that of the native enzyme, which justifies the assumption that both species act as catalysts in basically the same way. There are, however, certain differences in the chemical and enzymatic properties of different metallo-LADHs (6, 10, 12, 13, 15). For instance, Dunn *et al.* observed significant differences concerning spectral properties and rate parameters of substrate binding and turnover in ternary complexes of the general composition $Me(c)_2Zn(n)_2$LADH/NADH/*trans*-4-(*N*,*N*-dimethylamino)cinnamaldehyde, where Me = Co(II), Zn(II), Ni(II), and Cd(II) (13). Still, in their study the conclusion was drawn that, in metallo-ADHs used so far, the catalytic metal ion preserves tetrahedral coordination [with the possible exception of Cd(II)], and their different catalytic behavior reflects the different chemical properties of the metal

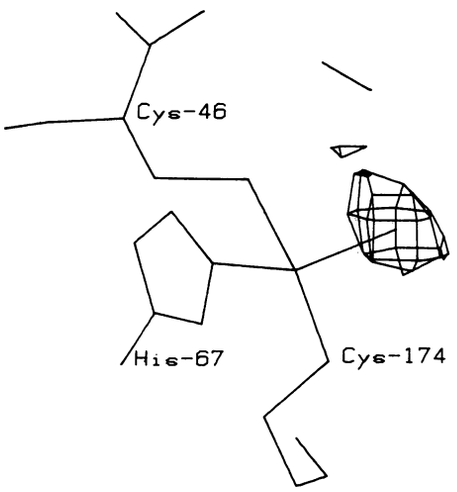

FIG. 6. Peak at the position of the metal-bound water molecule in $Co(c)_2Zn(n)_2$LADH; map with coefficients ($|F_{obs}| - |F_c|$).

Table 1. Comparison of bond angles between the ligands of each catalytic cobalt ion in $Co(c)_2Zn(n)_2$LADH and each catalytic zinc ion in the native enzyme

Atoms	Angle, degrees* Co(II)	Zn(II)†
S(Cys-174)—Me—N(His-67)	116	105
S(Cys-46)—Me—N(His-67)	100	112
S(Cys-46)—Me—S(Cys-174)	130	126
S(Cys-174)—Me—O(H_2O)	97	100
S(His-67)—Me—O(H_2O)	102	101
S(Cys-46)—Me—O(H_2O)	107	108

*The accuracy of the determination of the angles is estimated from the angles of the noncatalytic zinc sphere, coordinated to four sulphur atoms in a tetrahedral geometry. The root-mean-square deviation from a perfect tetrahedral coordination of this zinc ion is ±5° at the present resolution and stage of refinement.

†T. A. Jones, personal communication.

ions in virtually identical environments. It is obvious that comparison of crystal structures of different metallo-LADHs and their binary and ternary complexes with coenzyme and substrates (inhibitors) is needed; this information will form a valuable and necessary baseline to which differences in other chemical properties can be related.

We thank Dr. T. A. Jones for access to phase angles prior to publication. We appreciate the help of Dr. B.-O. Söderberg with our diffractometer system. One of us (G.S.) thanks Prof. C.-I. Brändén for all the facilities placed at his disposal in Uppsala. This work was supported by Deutsche Forschungsgemeinschaft, Fonds der Chemischen Industrie, and Grant 2767 from the Swedish Natural Science Research Council.

1. Sytkowsky, A. L. & Vallee, B. L. (1978) *Biochemistry* **17**, 2850–2857.
2. Sytkowsky, A. L. & Vallee, B. L. (1976) *Proc. Natl. Acad. Sci. USA* **73**, 344–348.
3. Sytkowsky, A. L. & Vallee, B. L. (1975) *Biochem. Biophys. Res. Commun.* **67**, 1488–1493.
4. Sytkowsky, A. L. & Vallee, B. L. (1979) *Biochemistry* **18**, 4095–4099.
5. Klinman, J. P. (1981) *CRC Crit. Rev. Biochem.* **10**, 39–78.
6. Maret, W., Andersson, I., Dietrich, H., Schneider-Bernlöhr, H., Einarsson, R. & Zeppezauer, M. (1979) *Eur. J. Biochem.* **98**, 501–512.
7. Maret, W., Dietrich, H., Ruf, H. H. & Zeppezauer, M. (1980) *J. Inorg. Biochem.* **12**, 241–252.
8. Dietrich, H., Maret, W., Kosłowski, H. & Zeppezauer, M. (1981) *J. Inorg. Biochem.* **14**, 297–311.
9. Andersson, I. (1980) Dissertation (Universität des Saarlandes, Federal Republic of Germany).
10. Shore, J. D. & Santiago, P. (1975) *J. Biol. Chem.* **250**, 2008–2012.
11. Andersson, I., Maret, W., Zeppezauer, M., Brown, R. D. & Koenig, S. H. (1981) *Biochemistry* **20**, 3424–3432.
12. Makinen, M. W. & Yim, M. B. (1981) *Proc. Natl. Acad. Sci. USA* **78**, 6221–6225.
13. Dunn, M. F., Dietrich, H., MacGibbon, A. H., Koerber, S. C. & Zeppezauer, M. (1982) *Biochemistry* **21**, 354–363.
14. Dunn, M. F. & Hutchinson, J. S. (1973) *Biochemistry* **12**, 4882–4892.
15. Dietrich, H. (1980) Dissertation (Universität des Saarlandes, Federal Republic of Germany).
16. Dalziel, K. (1957) *Acta Chem. Scand.* **11**, 397–398.
17. Eklund, H., Nordström, B., Zeppezauer, E., Söderlund, G., Ohlsson, I., Boiwe, T., Söderberg, B.-O., Tapia, O., Brändén, C.-I. & Åkeson, Å. (1976) *J. Mol. Biol.* **102**, 27–59.
18. North, A. C. T., Phillips, D. C. & Matthews, F. S. (1968) *Acta Crystallogr. Ser. A* **24**, 351–359.
19. Eklund, H., Samama, J.-P., Wallén, L., Brändén, C.-I., Åkeson, Å. & Jones, T. A. (1981) *J. Mol. Biol.* **146**, 561–587.
20. Jones, T. A. (1978) *J. Appl. Crystallogr.* **11**, 268–272.
21. Jones, T. A. (1982) in *Computational Crystallography*, ed. Sayre, D. (Oxford Univ., New York), pp. 303–317.
22. Brändén, C.-I., Jörnvall, H., Eklund, H. & Furugren, B. (1975) in *The Enzymes*, ed. Boyer, P. D. (Academic, New York), 3rd Ed., Vol. 11, pp. 103–190.